Influence of temperature on selenium mobility under contrasting redox conditions: a sediment flow-through reactor experiment.

Audrey Laberge-Carignan[1], Florence Mercier[1], Dominic Larivière[2], Raoul-Marie Couture[1]*

1- Université Laval, Department of chemistry, Center for Northern Studies (CEN) and Interuniversity Research Group in Limnology (GRIL) Université Laval, 1045 avenue de la médecine, Québec (Qc), G1V0A6, Canada
2- Université Laval, Department of chemistry and Center for Northern Studies (CEN) Université Laval, 1045 avenue de la médecine, Québec (Qc), G1V0A6, Canada

*Correspondance : raoul.couture@chm.ulaval.ca

Acknowledgements

We thank Lise Rancourt (INRS-ETE) and Serge Groleau for help with instrumental analysis. RMC acknowledges logistical support from the Center for Northern Studies (CEN), and funding from the Sentinel North program of Université Laval, Canada First Research Excellence Funds, and the National Science and Natural Sciences and Engineering Research Council of Canada through the Discovery Grant program. We acknowledge the Quebec Ministère de l'Environnement, de la lutte contre les changements climatiques, de la faune et des parcs for granting us access to the Tantaré ecological reserve. We thank M. Thaler for reviewing earlier versions of this manuscript.

Abstract:

We studied selenium (Se) sequestration in minimally disturbed lacustrine sediments using flow-through reactors (FTR) in response to organic matter lability, selenium (Se) speciation and temperature (4 and 23°C). Initial sediment was composed of either fresh or aged organic matter (OM), and was fed with environmentally relevant, low Se concentrations and filtered lake water. We monitored Se concentration as well as speciation along with pH and the concentrations of dissolved OM, NO_3^-, NO_2^-, Fe(II), SO_4^{2-} and HS^- in the outflow of FTRs during 8 experimental phases along increasing Se concentrations. All experiments sequestered a large proportion of Se. Fresh, labile OM removed 50% more Se than aged, more recalcitrant OM. Along with a highest proportion of reduced redox-sensitive species in the reactors with fresh OM, this result is consistent with reducing conditions promoting Se sequestration. Inflowing selenite was sequestered to a larger extent than inflowing selenate. Lastly, only selenate reduction responded strongly to temperature. At 100 nM inflow, selenate was sequestered at a rate of 92 pmol cm^{-3} d^{-1} at 23°C, which lowered to 80 pmol cm^{-3} d^{-1} at 4°C. Outflow Se speciation for selenate reduction experiments comprised mostly of organic Se species at 23°C and, in contrast, solely of selenate at 4°C. We hypothesize that selenate reduction proceeded via microbial processes, in line with reactions catalyzed by enzymes being temperature dependent. Overall, our findings suggest that the mobilisation and warming of the boreal and permafrost carbon pools may increase the capacity of aquatic environments to sequester Se, lowering its bioavailability.

Keywords:

Cold-region biogeochemistry; organic matter lability; temperature response; selenium speciation; reduction rates.

Introduction

Selenium is an essential micronutrient that has a narrow window of concentration between deficiency and toxicity (Hatfield et al. 2016). In surface waters, Se transfer to the food web is strongly influenced by sediment–water interactions (Martin et al. 2022), where sediments can be either sources or sinks of Se depending on the complex interplay between organic carbon lability, major redox, and microbially-mediated pathways (Laberge-Carignan et al. 2024). Freshwater sediments and water-logged soils are key features of cold-region landscapes worldwide. They are ubiquitous in vast expanses of the boreal (14 % of the land surface) and permafrost (11 % of the land surface) landscapes, as well as in large proportions of temperate ecoregions. Such wetlands, lakes and river systems are underlain by sediments that experience seasonal cooling under the influence of 4°C water which sinks and accumulate at the sediment-water interface throughout the cold season (Jones et al. 2024).

Seasonally alternating temperatures, organic matter (OM) and dissolved oxygen (DO) concentrations thus form the basis of hydrogeochemical and ambient redox conditions that impact Se speciation and mobility. Se is a redox sensitive element with four different redox states naturally found in the environment, -2, 0, +4 and +6 (Winkel et al. 2012). Selenate (SeO_4^{2-}), the oxyanion of Se(VI), is the most mobile Se species and the main species in oxic conditions (Sharma et al. 2015). Selenite ($HSeO_3^-$ or SeO_3^{2-}), the oxyanion of Se(IV), has a stronger affinity for adsorption onto clays and metal oxides such as ferrihydrite and gibbsite, onto which it form inner-sphere complexes (Deen et al. 2022; Fernández-Martínez & Charlet 2009; Goberna-Ferron et al. 2021). Selenite also as a stronger binding affinity than selenate for dissolved organic matter, which provides a pathway for its sequestration in sediment (Dalai et al. 2023; Sharma et al. 2015). Se species can adsorb onto pyrite, which leads to the reduction of selenate to selenite at the mineral's surface (Guida et al. 2023) and the reduction of selenite to $Se_{0(s)}$ (Deen et al. 2022; Mitchell et al. 2013). Pyrite yields higher selenite reduction rates compared to siderite and sphalerite (Deen et al. 2022), making it an important reactive surface in abiotic Se reduction (Guida et al. 2023). Ultimately, both selenate and selenite can be reduced to poorly soluble elemental $Se_{0(s)}$. Collectively, the above-mentioned abiotic processes, which are considered to be at

equilibrium, can nevertheless be hindered by dissolved OM (DOM) acting as a ligand, as previously shown for arsenic (As) adsorption onto Fe oxides (Couture et al. 2010).

OM is thus a key factor controlling Se speciation and mobility (Dalai et al. 2023; Gustafsson & Johnsson 1992), both as a ligand and as an electron donor during the sequential utilization of terminal electron acceptors. OM presenting a greater proportion of labile moieties such as polysaccharides, proteins, organic acids, fatty acids (Poirier et al. 2005) will establish microbial activity to along the redox gradient (LaRowe & Van Cappellen 2011), promoting electron transfer (Borch et al. 2010; Paredez et al. 2017). Given that microbial processes proceed via enzymatic reactions, their rate is constrained by temperature (Davidson et al. 2006; Nielsen et al. 2019). OM oxidation progressively leaves more recalcitrant OM, that can act as a ligand and complex dissolved Se (Gustafsson & Johnsson 1994; Li et al. 2017). In waterlogged soil and sediment, redox stratification responds to the availability of OM that is labile towards microbial oxidation (Vincent et al. 2024). Several mechanisms, often simultaneous, account for the interactions between Se and OM. These include microbial uptake and transformation (Luo et al. 2022), direct or indirect complexation (Martin et al. 2022; Sharma et al. 2015), and Se reduction under anoxic conditions, which are controlled by OM and temperature (Li et al. 2017; Nielsen et al. 2019; Tolu et al. 2014). Ultimately, biotic selenate and selenite reduction proceeds via either dissimilatory reduction to poorly soluble $Se_{0(s)}$ (Martin et al. 2011; Schilling et al. 2018), or assimilatory reduction to organo-Se, which is essential for life (Hatfield et al. 2016; Sharma et al. 2015).

The fate of Se in cold region is a concern in aquatic environments (Laberge-Carignan et al. 2024), agricultural settings (Pi et al. 2023), and under the influence of anthropogenic activities such as coal combustion (Cooke et al. 2024). Nevertheless, and despite cold-region being inherently characterised by 4°C water during the cold season, data on sediment Se dynamics are generally reported at growing season (e.g., room) temperature. It is likely that warmer temperature will affect the sediment's capacity to retain Se by enhancing microbially favorable pathways (Wells & Stolz 2020), the dissolved organic matter (DOM) composition and concentration (Porcal et al. 2015), the kinetics of chemical

reaction (Davidson et al. 2006), and the solubility of dissolved oxygen (DO) (Schladow et al. 2002).

In addition, a wide array of Se reduction rates are obtained from microbial pure culture experiments (Kausch et al. 2012; Luo et al. 2022; Yan et al. 2020), or sterile batch experiments (Dalai et al. 2023; Goberna-Ferron et al. 2021; Guida et al. 2023; López-Toyos et al. 2023), under conditions far from those prevailing in the field. Such experiments result in an artificially high reaction rates given the high supply of substrates for enzymatic reactions (Schilling et al. 2019; Schilling et al. 2018). Thus, there exists knowledge gap on the rate of Se sequestration at cold temperature in environmentally relevant conditions.

Here, we aim to fill this gap and provide a first estimate of the temperature control on Se sequestration under such environmentally relevant conditions, specifically: i) low, nM Se concentrations, ii) minimally disturbed sediment which preserves the microbial niches (Pallud et al. 2007; Pi et al. 2023) and iii) under both cold (4°C) and warm (23°C) conditions. This will allow a realistic estimate of the *in situ* apparent Se reaction rate, relevant for the field (Schilling et al. 2018). Further to cold and warm comparison, we also compared the role of OM lability as well as the behavior of both selenate and selenite as Se species fed to the FTRs. The former was achieved by selected initial sediment with abundant labile (*i.e.*, fresh) organic carbon supplied with dissolved oxygen, and sediment with recalcitrant (*i.e.*, aged) carbon under anoxic conditions, while the latter was achieved by adding either selenate or selenite to the input solutions and performing Se speciation measurements in the outflow. To our knowledge, this is the first study to report of naturally occurring Se reduction rate at both 4 and 23°C, two environmentally relevant end member of cold-region temperature.

Materials and Methods

Field site

The sediments used in the FTRs were sampled from the deepest point (21 m) of Lake Tantaré (47°04′15″ N, 71°33′42″ W). This dimictic freshwater headwater oligotrophic lake is located in an ecological reserve, 38 km northwest of Quebec City. The lake drainage basin has never been inhabited and is dominated by ferrohumic podzols (Liu et al. 2015).

Human activity impacts on the lake are solely from atmospheric deposition (Couture et al. 2008). The sampling site is characterized by seasonal anoxia at the sediment–water interface in late summer, 4°C hypolimnetic water, a pH around 5.6 and dissolved organic carbon (DOC) concentrations between 2.2 and 2.7 mg L^{-1}(Couture et al. 2008; Fortin et al. 1993; Joshani et al. 2024; Liu et al. 2015).

The sediment mass accumulation rate was 10.8 mg cm^{-2} yr^{-1} at the sampling site (Couture et al. 2008). Previous studies have shown that the composition (Joshani et al. 2024) and lability (Couture et al. 2010) of sedimentary OM vary with depth, where the surface OM being more labile (Fig. 1b). A large proportion of the sediment mineral phase is crystallized lepidocrocite (Fortin et al. 1993). At the sampling site, both the solid-phase and porewater concentration of Fe and trace elements are relatively constant with depth (Couture et al. 2008).

Sediment and Porewater Sampling.

A first core was retrieved in September 2020 with a 9 cm diameter gravity corer equipped with a core catcher (Uwitec, Austria) using a pre-drilled tube. This core was only used to withdrawn sediment porewater every cm from the sediment-water interface down to 10 cm depth using Rhizon samplers (Rhizosphere, Wageningen, Netherlands). The porewater was delivered into acid-washed 15 mL conical tubes containing HNO_3 (Aristar Ultra, VWR, Canada) yielding a final sample concentration of 4% HNO_3 for major and trace element analysis. In June 2022, three more cores were retrieved at the same site. One core was sliced every cm, freeze-dried and used as a sediment reference for initial conditions. The two other cores were used to assemble the FTRs.

Flow-Through Reactor Experiments Setup

A Plexiglas® ring 2 cm high with a 4 cm internal diameter was inserted in the middle of a sediment layer to retrieve the sediment with minimal disturbance. The ring was capped with a 0.45 µm polyethersulfone membranes (VWR, Canada), a fiberglass backing filter (Adventec MFS, Inc., Ireland) and finally a plastic cover with a hole that allows liquid to circulate. The same assembly was then performed on the other side of the ring to encapsulate the sediment within the FTR (Couture et al. 2008; Pallud et al. 2007). The

FTRs were assembled in the field immediately after sampling and kept at 4°C in the dark until the start of the experiment.

Lake water was collected on the same day as the sediments, was filtered on a 0.45 µm polyethersulfone membranes (VWR, Canada) and used as a matrix to prepare input solutions. Inputs were spiked with Na_2SeO_4 (anhydrous, 99.8% metal basis, AlfaAesar, Canada) for selenate or Na_2SeO_3 (anhydrous, 99% metal basis, AlfaAesar, Canada) for selenite. Inputs were pumped through the FTR using a peristaltic pump (IPC, Ismatec, Germany) at a constant flow rate of 1.0 ± 0.1 mL h^{-1}, which represents one FTR volume per day.

Pairs of FTRs (F and A) were placed in temperature-regulated bath (Refrigerated circulating bath, Thermo SC100) and isolated from light. The baths were set to cold (4°C) or warm (23°C) temperature, yielding 4 simultaneous FTR experiments. Each experiment lasted through two experimental phases, which started after an acclimatization of 14 days. The acclimatization phase was carried in the same conditions has the ones used for the following phases of the experiment. The two phases impose selenate (SeO_4^{2-}) or selenite ($HSeO_3^-$) in the inflow (Table 1). At the end of the last phase, inflow Se concentrations were increased to 2 µM with SeO_4^{2-} in the F FTR and 2 µM with $HSeO_3^-$ in the A FTR for the last 10 days of the experiments.

Table 1 : Lability of organic carbon, experimental temperature, selenium inflow species and their concentrations in the 2 experimental phases of each of the 4 reactors.

Organic matter	Temperature (°C)	Se species	[Se](nM)	Label
Fresh, labile	4	$HSeO_3^-$	7	Cold-F-4
Fresh, labile	4	SeO_4^{2-}	100	Cold-F-6
Aged, recalcitrant	4	$HSeO_3^-$	100	Cold-A-4
Aged, recalcitrant	4	SeO_4^{2-}	70	Cold-A-6
Fresh, labile	23	$HSeO_3^-$	7	Warm-F-4
Fresh, labile	23	SeO_4^{2-}	100	Warm-F-6
Aged, recalcitrant	23	$HSeO_3^-$	100	Warm-A-4
Aged, recalcitrant	23	SeO_4^{2-}	70	Warm-A-6

Outflow solutions were collected using an automated fraction collector (Omnicoll, LAMBDA, Czech Republic) and delivered directly into the appropriate vials containing preservation reagents. Samples for major and trace element analyses were delivered into acid-washed 15 mL conical tubes containing HNO_3 (Aristar Ultra, VWR, Canada) yielding a final sample concentration of 4% HNO_3. Due to the possibility of Fe flocculation with DOC in the sample, the Fe concentrations were also confirmed by the ferrozine method to ensure the total recovery of Fe(II) (Li et al. 2024). Samples for Se speciation were delivered using a needle directly into N_2-purged vials, and those for sulfide analysis into an N_2-purged glass vials amended with Zn-acetate (Thermoscientific, USA). Finally, samples for anion analysis were delivered to HDPE ion chromatography vials (Thermoscientific, USA).

Instrumental analysis

The major and trace element concentrations in the outflow solutions were analyzed weekly. Major elements (Na, Ca, Mg, K, S, Fe, Mn) were quantified by inductively coupled plasma atomic emission spectrometry (ICP-AES, Thermo Scientific duo iCAP 7400) with iridium (Ir) as an internal standard. Selenium (Se) concentrations were determined by ICP-MS/MS (Agilent 8900, Agilent Canada) with rhodium (Rh) as an internal standard. To avoid interference from $^{40}Ar_2^+$, we used O_2 as a reaction gas and measured the polyatomic $^{78}Se^{16}O^+$ ion. For all measured elements, the difference between the measured (n = 5) and the certified values for certified material TM-DWS.3 (Filtered Lake water, ECCC, Canada) was less than 10 %.

Se speciation of the outflow solution was carried out by HPLC-ICP-MS/MS (Agilent 8900). Fifty µL of sample was eluted through a Hamilton PRP X-100 (4.1 mm × 250 mm, 10 µm) column with 10 mM of ammonium acetate, pH = 4.9 in MeOH 2% at 1 mL min^{-1} (Gao et al. 2018). ^{77}Se was monitored with a 5 mL min^{-1} H_2 flow in the reaction cell to diminish interference. External calibration was performed between 0 and 5 µg L^{-1} for SeO_4^{2-} and $HSeO_3^-$ ($R^2 > 0.999$).

The difference between the total Se concentration obtained by ICP-MS/MS and the sum of selenate and selenite concentrations is assumed to include undefined Se species. To ascertain the nature of the Se species that covers of that difference, we have performed a

UV oxidation test on a sample from the Warm-F FTR outflow (Chen et al. 2005), which shown a quantitative increase in Se after oxidation of the sample. This strongly suggest that the Se balance is organic, although we could not identify the structures of the compounds prone to UV oxidation. Thus, the difference between the sum of the inorganic species concentrations and the total Se concentration is understood to be undefined Organo-Se species (Martin et al. 2011; Ponton & Hare 2013).

The fractions for anion (NO_2^-, NO_3^-, SO_4^{2-}, $S_2O_3^{2-}$) analysis were collected at the beginning and the end of each phase, except for the two phases of the Warm-F FTR for which we only have one sample. Anions were measured by ion chromatography (Integrion IC, ThermoFisher, USA) equipped with a AS11-HC column, with a detection limit below 0.1 µmol L^{-1} for all anions. HS^- and Fe(II) were quantified by UV-VIS colorimetry (Aqualog, HORIBA Scientific, USA) using the Cline (Cline 1969) and the ferrozine (Viollier et al. 2000) method, respectively. The detection limits was 0.7 µmol L^{-1} for HS^- and 0.03 µmol L^{-1} for Fe(II).

The effluent DOC quality was characterized by fluorescence excitation emission matrices (EEM) on a spectrofluorometer (Aqualog, HORIBA Scientific, USA), at an excitation range of 240–800 nm in steps of 5 nm, with an emission range of 240–800 nm in steps of 5 nm. The EEM spectra were used to calculate three optical indices: the fluorescence index (FI), the freshness index (BIX) and the humification index (HIX) (Gabor et al. 2014; Ohno 2002; Shatilla & Carey 2019; Wilson & Xenopoulos 2009). Details on the calculation of the different indices are provided elsewhere (Laberge-Carignan et al. 2024).

After the acquisition of EEM spectra, the samples were acidified with HCl to quantify dissolved organic carbon (DOC) and total dissolved nitrogen (TDN) using a Vario TOC-Cube TOC analyzer (Elementar, Germany) coupled to a Horiba NO_x analyzer (Horiba Scientific, USA). The detection limits were 20 µM for DOC and 10 µM for TDN.

Sediments collected prior and after FTRs experiments were freeze-dried and ground with an agate mortar and pestle. The sediments were mineralized by microwaves (Mars 5, CEM Canada) with concentrated acid (trace metal, VWR, Canada) in Teflon vessel as detailed in the supporting information (Lizotte et al. 2023). Each sample was mineralized in triplicate.

The major and trace elements were analyzed in the mineralized solutions as described above.

Data Analysis

The selenate and selenite reduction rates (R_{Se_net}; pmol cm^{-3} d^{-1}) were calculated as:

$$R_{Se\_net} = \frac{(C_0 - C_{out})Q}{V} \qquad (1)$$

Where: C_0 (mol cm^{-3}) is the inflow SeO_4^{2-} or HSO_3^- concentration, C_{out} (mol cm^{-3}) is the outflow SeO_4^{2-} or $HSeO_3^-$ concentration as provided by Se speciation analysis, Q is the inflow rate (cm^{-3} d^{-1}) and V (cm^{-3}) is the FTR volume (Pallud et al. 2007; Steinberg & Oremland 1990). Dissolved Se efflux (J; mol L^{-1} d^{-1}) was calculated by dividing the slope (mol d^{-1}) of the cumulative Se outflow concentration as a function of time by the volume (cm^3) of the reactor. The assumptions that both the one-dimensional flow and the concentrations in the sediment slices are radially homogenous underpins the interpretation the outflow data in terms of kinetic parameters (Pallud et al. 2007). This is reasonable assumption given the features of the bromide breakthrough curves in such minimally disturbed sediment (Couture et al. 2013).

In data interpretation, we focus on the net Se reaction rates, and do not evaluate the maximum potential reduction rate or the half-saturation constant for enzymatic selenite and selenate reactions. Because R_{Se_net} is dependent on the C_0 (Steinberg & Oremland 1990), we calculate normalized rates (NR_{se_net}; mol L^{-1} d^{-1}) to enable comparison between experiments with different inflow concentrations from the literature, using the following equation:

$$NR_{Se\_net} = R_{Se\_net} \times \frac{C_{0\_max}}{C_0} \qquad (2)$$

Where: C_{0_max} is the maximal inflow Se concentration (100 nmol cm^{-3}).

Finally, the redox conditions prevailing in the FTRs were calculated based on theoretical standard reduction potential values, measured pH and cations and anion concentrations as well as the measured redox couples Fe^{3+}/Fe^{2+}, NO_3^-/NO_2^- and SO_4^{2-}/HS^-. All concentrations were measured except for Fe^{3+} whose concentration is calculated with PHREEQC assuming an equilibrium with $Fe(OH)_{3(s)}$ (Couture et al. 2013).

Thermodynamic calculations were performed with the public domain computer code PHREEQC, Version 3.8.3 (Parkhurst & Appelo 2013), the thermodynamic database PHREEQC.dat imbedded with PHREEQC and an input file suitable for redox potential calculations (Saaltink & Rodríguez-Escales 2022) modified with the SOLUTION_SPREAD keyword.

Results and Discussion:

Preliminary Data Prior to the FTR Experiments

Table 2 : Quantitative characterisation of the sediment used in the flow through reactor containing fresh (0-2 cm) and aged organic matter (8-10 cm).

Variable	Unit	Value	
		0-2 cm	**8-10 cm**
Porosity	-	0.97	0.95
Water content	%	95	91
Organic C	%	25	23
Organic N	%	1.6	1.1
OM mineralization rate	$\mu m\ cm^{-3}\ yr^{-1}$	465	80
Solid-phase Fe	$\mu mol\ g^{-1}$	267	307
Solid-phase Se	$nmol\ g^{-1}$	17	23
Porewater Se	nM	0.7	1.2
Porewater Fe	µM	143	153
Porewater NO_3^-	µM	1.4	2.0
Porewater SO_4^{2-}	µM	0.5	0.1

Two sets of observations (Couture et al. 2008; Couture et al. 2010; Fortin et al. 1993; Joshani et al. 2024; Liu et al. 2015), summarized in Table 2, were used to set experimental conditions, in addition to the imposed FTR temperature. Firstly, dissolved Se increased sharply below the sediment–water interface, then remained relatively stable throughout the profile with *in-situ* porewater Se concentration within the nanomolar range, from 0.7 nM at the sediment–water interface to a maximum of 1.2 nM at a depth of 4 cm in the sediment (Fig. 1a).

Second, the lability (e.g, quality) of the OM was estimated via incubations that yielded OM mineralization rates (Couture et al. 2010). OM degradation rates decreased from 465 µmol $cm^{-3}\ yr^{-1}$ below the sediment–water interface to lower than 80 µmol $cm^{-3}\ yr^{-1}$ at 10 cm

depth (Fig. 1b). Thereafter, the 0–2 cm sediment layer was selected for FTRs with high OM oxidation potential (fresh labile OM, FTRs labeled F) and the 8–10 cm layer was selected for FTRs with low OM oxidation potential (aged recalcitrant OM, FTRs labeled A). ^{210}Pb dating of the cores are the sampling site indicate that the fresh labile OM is less than six years old and the aged recalcitrant OM around 50 years old (Couture et al. 2008).

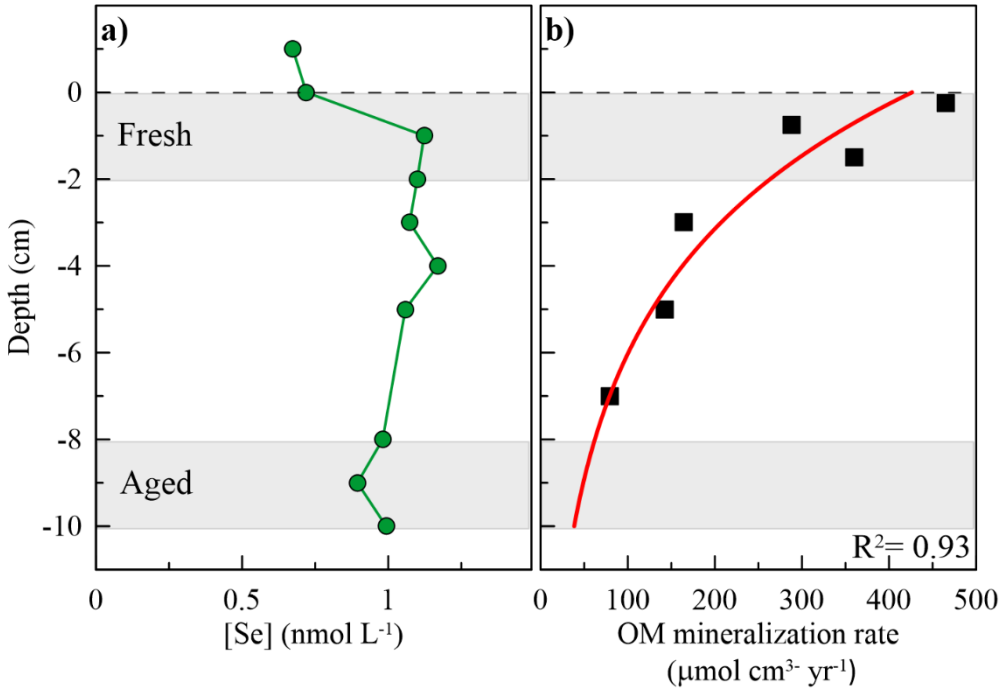

Fig. 1 Porewater Se concentration profile (green circles) in Lake Tantaré sediments (panel a; this study) and depth profile of organic matter mineralization rate derived from the measured CO_2 accumulation in the headspace of oxic incubated slurries (squares), and the function describing its exponential decline with depth (red line; panel b; (Couture et al. 2010). The horizontal dashed line represents the sediment–water interface and the gray zones the depths sampled for the reactor experiments, here after labeled Fresh (F) and Aged (A).

Outflow Selenium Concentrations During FTR Experiments

Outflow Se concentrations reached various plateaus depending on the experiment (Fig. 2). The highest values of 8–12 nM were reached within 2 days for the two cold FTRs with selenate as inflow Se species. The two other selenate-fed FTRs and all the selenite-fed FTRs had outflow Se concentrations between 0.7 and 4.5 nM, respectively, thus sequestering more Se.

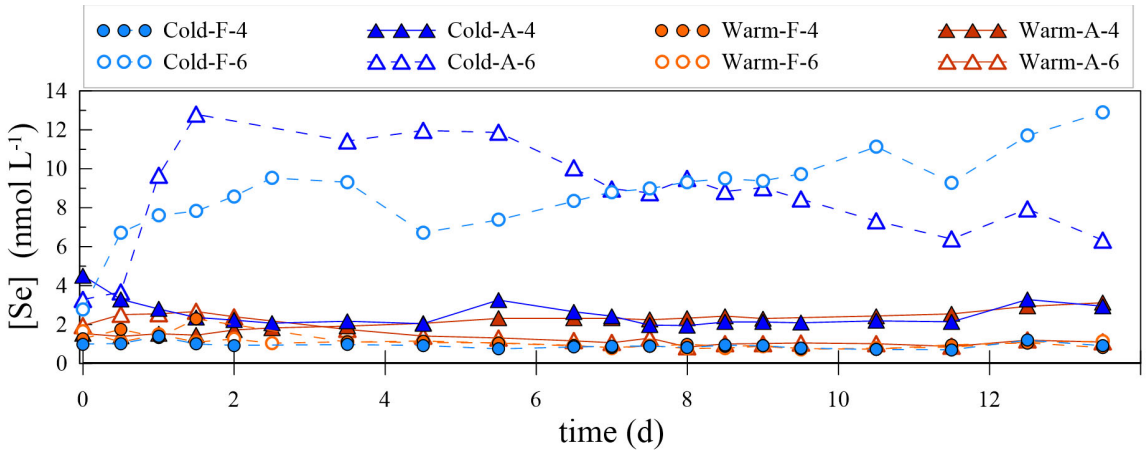

Fig. 2 Outflow Se concentration ([Se]; nmol L^{-1}) as a function of time (d) for each experiment. Blue and orange indicate cold (4°C) and warm (23°C) reactors, respectively. Lighter colored circles represent experiments with fresh OM (F) and darker colored triangles represent experiments with aged OM (A), while solid and open symbols indicate respectively selenite and selenate as inflow Se species.

For the warm FTRs fed with selenate, the majority of Se in the outflow solution was comprised of these undefined Se species, with the balance composed of 20 % selenate and 10 % selenite, for example in the Warm-A FTR (Supplementary Information Figure S4, S7). In contrast, inorganic Se species dominated the outflow Se speciation in the cold FTRs, with mostly selenate being measured (Supplementary Information Figure S4). For the experiments fed with selenite, the majority of Se in the outflow of all FTRs were undefined organic-Se species (Supplementary Information Figure S6).

Normalized selenate and selenite reduction rates (NR_{Se_net}; mol cm^{-3} d^{-1}) were calculated with the Se outflow concentration plateaus for each experiment that was fed with Se concentrations in the nanomolar range (Eq. 2; Fig. 3a). For the experiments with selenate, $NR_{Se\_net\_6}$ values were similar for both warm FTRs at 0.095±1 nmol cm^{-3} d^{-1}, and higher than the values for the cold FTRs (0.063 nmol cm^{-3} d^{-1}). For the experiments with selenite, the calculated $NR_{Se\_net\_4}$ values were similar for all FTRs, at 0.095±1 nmol cm^{-3} d^{-1}.

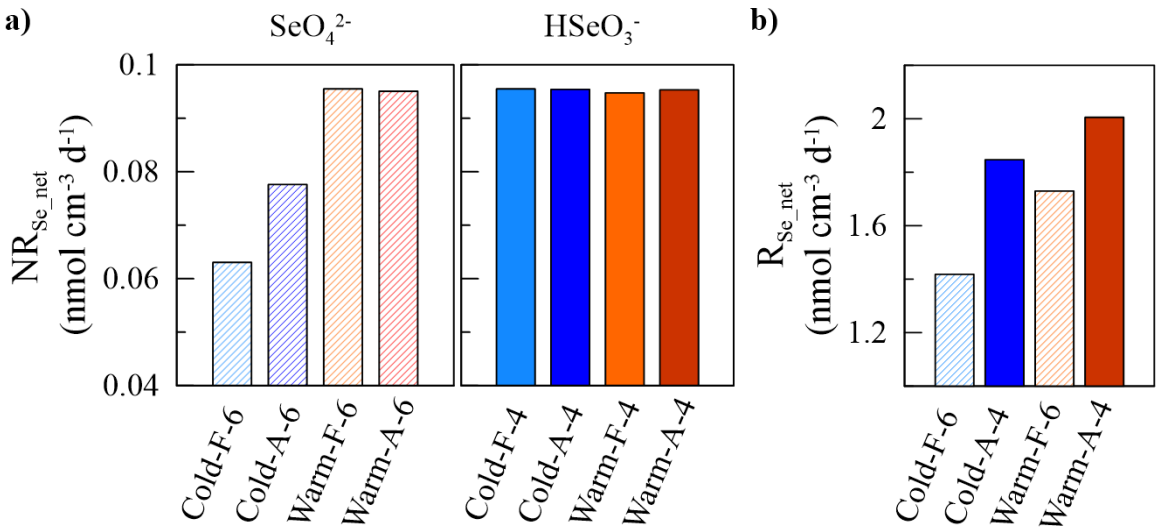

Fig. 3 Normalized potential selenite and selenate reduction rate (NR_{se_net}; nmol cm^{-3} day^{-1}) (panel a) and Se reduction rate (R_{se_net}; nmol cm^{-3} day^{-1}) for each FTR with an inflow Se concentration of 2 µM (panel b). Blue and orange bars indicate cold (4°C) and warm (23°C) reactors, respectively, while solid and hatched fill indicate selenite and selenate as inflow Se species, respectively.

Upon increasing the inflow Se concentration by 20-fold, selenate and selenite reduction rates (R_{Se_net}; nmol $cm^{-3}d^{-1}$) were calculated for each experiment (Equ. 1). The $R_{Se\_net\_6}$ values were calculated in FTRs with fresh OM and the $R_{Se\_net\_4}$ in the FTRs with aged OM. Selenate rates ($R_{Se\_net\_6}$) were lower than selenite rates ($R_{Se\_net\_4}$). The cold reactors had lower R_{Se_net} than the warm reactors (Fig. 3b).

Effect of OM Lability on Se Reduction Rates and Ambient Redox Potential

The quality of dissolved OM leached from the reactor was assessed using DOC and TDN analysis, as well as by measuring chromophoric properties of DOC to calculate the indices described above. DOC was generally under 2 mM, with TDN an order of magnitude lower, around 0.2 mM. The Cold-A reactor stood out, leaching up to 19 mM DOC and 2 mM TDN. In general, inflow and outflow values of FI, BIX and HIX point to inflow and outflow DOC being markedly different for the warm FTRs, and, in contrast, very similar for the cold FTRs (Supplementary Information Figure S8 and S9).

Among the warm FTRs, the FTR with fresh OM leached DOC that was more terrestrial, older and more humic compared to the FTR with aged OM, and to the initial solution. These changes in chromophoric properties suggest microbial degradation of the labile constituents of the sediment OM (Paredez et al. 2017). The remaining recalcitrant carbon

is leached out of the FTR, explaining the differences observed between the two warm FTRs.

Fig. 4 displays the mean ratios of the key redox couples NO_3/NO_2, Fe(III)/Fe(II) and SO_4^{2-}/HS^- in the reactor outflows. The experiments with fresh OM yielded systematically lower ratios of oxidized to reduced species for the major redox couples than the experiments with aged OM. Lower nitrate, sulfate, and iron(III) hydr(oxide) concentrations indicates redox biogeochemical reactions involving microbial activities (Bethke et al. 2011; Borch et al. 2010). The PHREEQC-calculated Eh values are consistent with this, where Eh is more reducing in the FTR with fresh OM and more oxidizing in the FTR with aged OM. For the FTR with fresh OM the main electron acceptor is SO_4^{2-} while Fe(III) is the main electron acceptor in the FTR with aged OM.

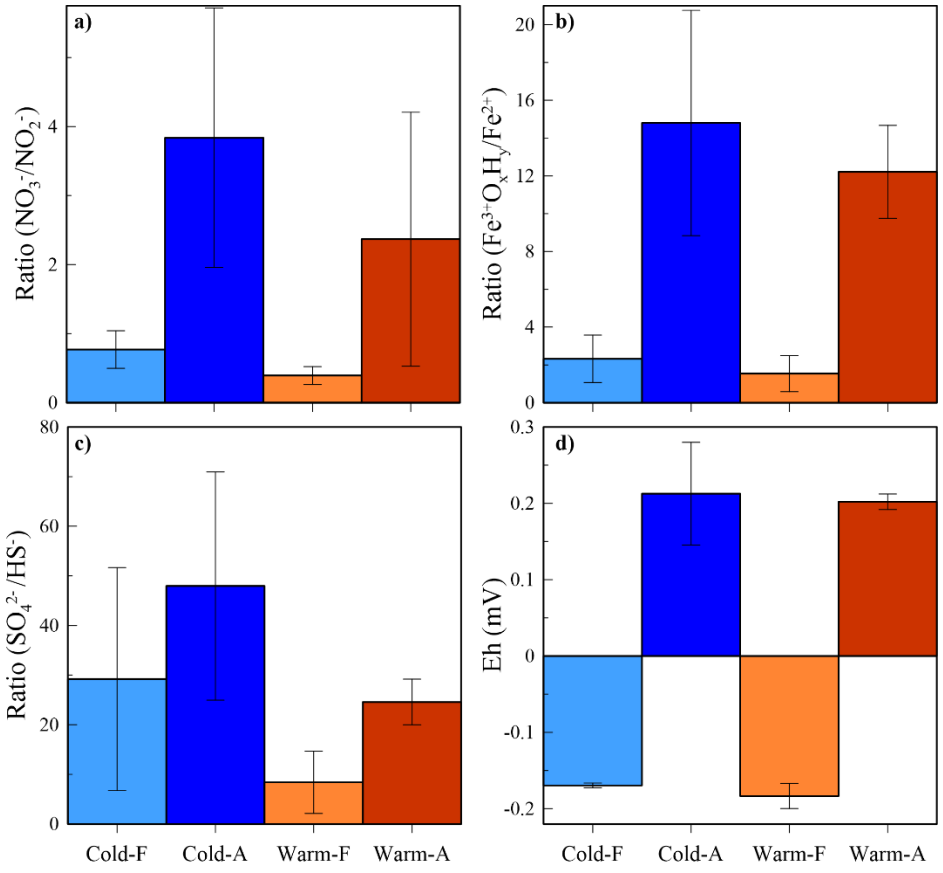

Fig. 4 Measured average ratio of oxidized to reduced species for nitrogen (NO_3^-/NO_2^-), sulfur (SO_4^{2-}/HS^-), and iron (Fe(III)/Fe(II)) along with calculated Eh for each experiment, along with standard deviation. Blue indicate cold (4°C) and warm indicate warm (23°C) reactors, while light and dark fill indicate fresh (F) and aged (A) OM, respectively.

Redox conditions affect the major redox couples and Se speciation, since microorganisms can reduce selenate or selenite to less mobile species ($Se^0_{(s)}$, Se(-II)) (Tolu et al. 2014). Among the warm FTRs, the one with fresh OM produced a lower proportion and concentration of oxidized Se species compared to the FTR with aged OM (Supplementary Information Figures S3-S6). The cumulative outflow Se plot (Supplementary Information Figure S1) was used to determine the dissolved Se efflux (J_{Se}; nmol L^{-1} d^{-1}) for each experiment (Supplementary Information Figure S2). The FTRs with fresh OM let through less Se than the ones with aged OM, consistent with previous studies on the effect of OM on Se sequestration (Calderone et al. 1990; Pi et al. 2023; Schilling et al. 2018; Tolu et al. 2014). In particular, Schilling et al. (2018) conducted FTR experiments to assess selenate reduction rates at different sediment depths, and observed higher $R_{se\_net\_6}$ at the sediment–water interface, which was associated with increased lability of OM, compared to deeper sediments.

The Gibbs free energy yield for the oxidation half reaction of OM ($\Delta G_{C\ ox}°$) is more negative for fresh OM than for aged OM (LaRowe & Van Cappellen 2011). Here, FTRs where high free energy yield was expected due to the abundance of fresh OM and faster experimentally-derived OM degradation rates (Couture et al. 2010) led to a wider range of values for OM chromophoric properties (Supplementary Information Figure S9), lower ratios of oxidized to reduced species for the major redox couples (Fig. 4), and lower Se effluxes (Supplementary Information Figure S2).

Influence of Temperature on Se Reduction Rates

Based on the DOC chromophoric properties (Supplementary Information Figure S9), the warm FTRs leached more terrestrial, old, and humic DOC compared to the inflow solutions. The cold FTRs did not exhibit this behavior. This is probably the outcome of enhanced enzymatic activity and OM decomposition under warmer conditions (Dick 2011). Similarly, the warm FTRs induced lower ratios of oxidized to reduced species for the major redox couples (Fig. 4) regardless of the lability of OM, indicating greater microbial activity.

Microbial reduction of selenate, which leads to Se removal via $Se^0_{(s)}$ particulate formation or incorporation into organic compounds (Fernández-Martínez & Charlet 2009), and Se

methylation are all known to be an enzymatic processes (Dick 2011). Increased temperature increases kinetic energy, facilitating enzymatic reactions, particularly in bacteria (Becker 1986; Davidson et al. 2006; Dick 2011). Microbial enzyme-catalyzed reactions are thus temperature-dependent, and their rate can double with each 10°C rise in temperature (Davidson et al. 2006). Indeed, at ambient temperature, published FTR experiments on Se reduction (Schilling et al. 2018) show that selenate-reducing capacity of the microbial communities are never exceeded. Here, the higher Se reduction rates (Fig. 3) for the warm FTRs compared to the cold FTRs are suggestive of microbial enzyme-catalyzed reactions. Microbial control is also explained by our observed variation in the proportion of organic Se species in the outflow solution between the warm and cold FTRs fed with selenate.

Söderlund et al. (2016) conducted batch experiments with selenite and selenate under aerobic conditions to assess the impact of temperature on Se removal. They observed low selenate removal, no speciation variation, and no temperature effects from 4 to 38 °C. Under aerobic conditions, selenate reduction is not favorable (Borch et al. 2010; Fernández-Martínez & Charlet 2009). Poor adsorption of selenate on mineral surfaces and low complexation with OM explain the observations reported by Söderlund et al. (2016). However, here the use of FTRs with undisturbed sediment that preserved microbial niches, and the anoxic conditions likely facilitated selenate reduction and removal (Schilling et al. 2018).

Contrasting Response of Selenite and Selenate to Experimental Conditions

All the FTRs fed with selenite had similar normalized rates (NR_{Se_net}; Fig. 3a). The lack of a temperature influence on the FTRs fed with selenite suggest abiotic removal reactions. As shown in the literature, abiotic Se reduction is not dependent on temperature (Söderlund et al. 2016). Bruggeman et al. (2007) observed selenite reduction to organically bound Se species by humic substances in abiotic laboratory batch experiments. Similarly, Dalai et al. (2023) showed selenite removal by abiotic interactions with OM, which were explained by the presence of Fe. In contrast, microbial selenate reduction is known as a primary Se removal pathway (Wells & Stolz 2020), with its reduction by abiotic pathways being slow

(Dalai et al. 2023) or absent (Bruggeman et al. 2007; VillaRomero et al. 2013) depending on the nature of the sediment.

We hypothesise that selenite is removed predominantly via abiotic pathway, while selenate is removed predominantly via biotic pathways. Our hypothesis is based on the observation that OM- and Fe-rich sediments remove selenite ($\leq$ 0.1 µM) rapidly and irrespective of either temperature or OM lability, as shown by the similar $NR_{Se\_net\_4}$ values between FTRs. In contrast, selenate seems to be controlled by biotic pathways, consistent with the decrease in $NR_{Se\_net\_6}$ alongside a decrease in temperature (Fig. 3a). This could be ascribed to an additional step needed in the reduction of selenate: most pathways for selenate reduction to Se_0 involve a two-step process where selenate reduction to selenite is followed by selenite reduction to organo-Se or $Se_{0(s)}$ (Wells & Stolz 2020).

Previous studies reported maximal selenate reduction rates based on a regression of potential rate as a function of the selenate input concentrations, following a Michaelis-Menten equation (Schilling et al. 2018; Steinberg & Oremland 1990; VillaRomero et al. 2013). Those microcosms were not Se-limited, as the authors insured that selenate was the sole terminal electron acceptor provided to the microbial community (Pallud & Van Cappellen 2006; Steinberg & Oremland 1990; VillaRomero et al. 2013). Here, other electron acceptors remain more abundant, such as the Se is a micronutrient and uptaken for assimilatory purposes. Rates derived are thus representative of in-situ environmental rates pertaining to cold regions, but not of the maximum potential for Se reduction of the sediment. Those reaction rates are lower for selenate ($R_{Se\_net\_6}$) than for selenite ($R_{Se\_net\_4}$) (Fig. 3b).

Net Selenium Reaction Rates Compared to Literature Data

Different Se reaction rates associated with sediments, solid phase or incubations are reported in the literature. Some authors refer to Se reduction rates as the rate at which the selenium is reduced to $Se_{0(s)}$ and sequestered in the solid phase by microorganisms (Lenz et al. 2008; Schilling et al. 2018; Steinberg & Oremland 1990). Others refer to removal rates, which are the selenium retention rate on the solid phase (Negi et al. 2020; Thompson et al. 2003). In this paper, we distinguish between these types of reduction rates. The Se

reaction rates (R_{Se_net}) reported in the literature stem from laboratory experiments conducted at ambient temperatures ranging from 15 to 35°C.

We conducted a systematic literature review according to criteria shown on Supplementary Information Figure S18. We found 8 studies reporting Se reduction or removal rates from natural sediments or soils with inflow Se concentrations ranging from nM to mM, and no study reporting results at low temperature. The reported R_{Se_net} values range from 0.0024 to 7080 nmol cm^{-3} d^{-1}, depending on the sediments used, the inflow concentrations, and the microbial communities involved (Table 3).

There is thus a paucity of published data on selenite removal, reduction or sequestration rates from laboratory or field experiments involving natural sediments or soils. Most available studies on selenite removal are based on batch experiments which did not reported rates (Table 3) (Darcheville et al. 2008; Li et al. 2015; Paredez et al. 2017; Söderlund et al. 2016; Tolu et al. 2014). Deen et al. (2022) conducted abiotic batch experiments to assess the adsorption capacities of selenite and selenate on various minerals. They reported selenite reaction rates ranging from 0.02 to 0.58 nmol $cm^{-3}d^{-1}$ at Se concentrations between 8.8 and 12.6 µM, except with pyrite where the selenite reaction rate was markedly higher, reaching 187 nmol $cm^{-3}d^{-1}$. Our FTRs experiments had selenite reduction rates between 1.8 and 2 nmol $cm^{-3}d^{-1}$ at an inflow concentration of 2 µM. The higher rates observed in our study may be attributed to the presence of microorganisms and OM in our system.

Literature values for R_{Se_net} are related to the inflow concentrations (Steinberg & Oremland 1990). Thus, for the sake of comparison, we calculated normalized rates (NR_{se_net}) (Eq. 2) obtain from similar experimental conditions using natural sediments or soils (Supplementary Information Figure S18). The rate obtain from our experiments are in the same order of magnitude as those reported for other lake sediments with low Se, yet lower than those from agricultural soils and pond sediments (Table 3).

Table 3 : Compilation of selenate removal or reduction rates reported in laboratory experiments with natural sediments or soils in the literature.

Authors	Temp. (°C)	Inflow Se (μM)	Type	Solid-phase	R_{Se_net} (nmol cm^{-3} d^{-1})	NR_{Se_net} (nmol cm^{-3} d^{-1})
Steinberg and Oremland (1990)	25	25	Batch	Hypersaline lake sediments	1.68[b]	0.01
Steinberg and Oremland (1990)	25	25	Batch	Hypersaline lake sediments	5.04[b]	0.02
Schilling et al. (2018)	25	96–765	FTR	Hypersaline lake sediments	21.6–492[b]	0.06
This study	4	0.07–0.10	FTR	Freshwater lake sediment	0.05–0.06	0.07
This study	4	2	FTR	Freshwater lake sediment	1.4	0.07
This study	23	2	FTR	Freshwater lake sediment	1.7	0.09
This study	23	0.07–0.10	FTR	Freshwater lake sediment	0.07–0.09	0.10
Steinberg and Oremland (1990)	25	25	Batch	Freshwater reservoir sediments	45.84[b]	0.18
Ho et al.(2022)	21	5	Column	Alluvial floodplain deposits	12[a]	0.24
Pi et al.(2023)	20	0.86	FTR	Organic rich mollisol	2.18[c]	0.25
Oremland et al. (1991)	20–26	0.30–0.37	Batch	Agricultural pond/drain sediments	0.89–1.19	0.32
Oremland et al. (Oremland et al.)	20–26	0.01-0.025	Batch	Freshwater lake sediment	0.012-0.149	0.60
Steinberg and Oremland (1990)	15	25	Batch	Agricultural pond/drain sediments	255.6[b]	1.02
Oremland et al. (1991)	20–26	0.038–0.051	Batch	Agricultural pond/drain sediments	0.22–0.55	1.08
Villa-Romero et al. (2013)	21	500	Batch	Hypersaline lake sediments	672–7080[b]	1.42
Oremland et al. (1990)	22	0.012–6.510	Batch	Agricultural pond/drain sediments	0.19–8.76	1.58
Steinberg and Oremland (1990)	25	25	Batch	Agricultural pond/drain sediments	529.68[b]	2.12

[b]Maximum potential selenate reduction rate

[c]Calculated rate from the publish values

The literature review shows that sediment with greater OM and nutrient content (e.g. agricultural sediment) have higher NR_{Se_net} than the hypersaline sediments. Many of the cited paper in the Table 3 evaluated the rate at different depth and concluded that the OM content was the main parameter influencing the selenate reduction rates.

Experiment geometry appear to play a role in the reduction rates obtained, batch yielding faster rates than either columns or reactors. VillaRomero et al. (2013) and Schilling et al. (2018) used sediments from the littoral site of the same lake, in similar condition, but obtain different rates (Table 3). Those variation are probably du to the increase in contact area between the sediment and the solution in batch experiments.

In the FTR experiment, the NR_{se_net} increase with the content in organic matter, from hypersaline lake sediment to organic rich mollisol (Table 3). Pi et al.(2023) conducted flow-through experiments with undisturbed mollisol, fed with 860 nM of selenate but did not report reaction rates. Using their data, we calculated a $R_{Se\_net\_6}$ of 2.18 nmol cm^{-3} d^{-1} for their 15 cm depth FTR. Mollisols showed higher NR_{Se_net} compared our freshwater lake sediments, probably due to their higher content in fresh and labile OM (Pi et al. 2023).

Thus, the warm FTR with fresh labile OM showed the highest Se removal capacity, with a stable Se efflux (0.94 nmol d^{-1} L^{-1}) regardless of changes in the inflow concentration or Se speciation (Supplementary Information Figures S2-S16-S17). Solid-phase Se concentrations more than tripled following the experiment in this FTR, leading to the highest Se concentrations in the sediment (161.8 ± 0.5 µmol kg^{-1}) (Supplementary Information Figure S15). Based on these results, we conclude that Se sequestration is faster in aquatic system rich in labile OM as temperature increases, by about 2-fold. This conclusion supports the field-derived calculation that Se flux from the sediment increase between the winter and the summer time (Laberge-Carignan et al. 2024).

Environmental relevance and transferability of the results

As many before us, we determined selenate removal rate in sediments. The literature review (Table 3) highlights the lack of experiment on selenite removal in environmentally relevant conditions and the lack experiment at low temperature (e.g. 4 °C). It does show, however, the OM plays a key role on selenate removal.

This experiment aimed to assess the impact of temperature and OM content on the mobility of selenite and selenate in sediments using FTRs. Surface sediments with labile, fresh OM removed 50% more Se than sediment with more recalcitrant OM. FTRs with fresh OM produced lower dissolved Se efflux along more reduced electron acceptor, and more degraded DOC in their outflows, suggesting higher microbial metabolism.

While temperature had little effect on selenite mobility at low concentrations, it significantly impacted selenate sequestration rates which decreased by more than 50 % under cold temperature. To our knowledge, this is the first experiment to evaluate Se mobility starting with selenate or selenite at temperatures lower than 15°C. We hypothesize that the difference points to two distinct reduction pathways: an abiotic pathway that reduces selenite, which is less affected by temperature, and a microbial pathway that reduces and sequesters selenate which is affected by temperature. Cold region soils are thus likely to increasingly retain Se. Those soils include peatlands in permafrost landscape, organic-rich lake sediments and organic-rich cryosols susceptible to warming under climate change. As a result, Se fluxes to the aquatic environment may decrease, while the risk of Se deficiencies throughout the food web may increase.

Supplementary Information

Additional details on methods, supporting results for pH, N, S, Fe and DOC concentrations, selenium speciation results, supporting statistical tests, and the literature review methodology (PDF).

Statements and Declarations

This work was supported by the funding from the Sentinel North program of Université Laval, Canada First Research Excellence Funds, and the National Science and Natural Sciences and Engineering Research Council of Canada through the Discovery Grant program.

Authors contributions

The authors have no relevant financial or non-financial interests to disclose.

All authors contributed to the study conception and design. Material preparation, data collection and analysis were performed by Audrey Laberge-Carignan and Florence Mercier. The first draft of the manuscript was written by Audrey Laberge-Carignan and all authors commented on previous versions of the manuscript. All authors read and approved the final manuscript.

References

Becker WM (1986) The world of the cell. Benjamin/Cummings, Menlo Park

Bethke CM, Sanford RA, Kirk MF, Jin Q, Flynn TM (2011) The thermodynamic ladder in geomicrobiology. Am. J. Sci. 311(3): 183–210.https://doi.org/10.2475/03.2011.01

Borch T, Kretzschmar R, Kappler A, Van Cappellen P, Ginder-Vogel M, Voegelin A, Campbell K (2010) Biogeochemical redox processes and their impact on contaminant dynamics. Environ. Sci. Technol. 44(1): 15–23.https://doi.org/10.1021/es9026248

Bruggeman C, Maes A, Vancluysen J (2007) The interaction of dissolved Boom Clay and Gorleben humic substances with selenium oxyanions (selenite and selenate). Appl. Geochem. 22(7): 1371–1379.https://doi.org/10.1016/j.apgeochem.2007.03.027

Calderone SJ, Frankenberger WT, Parker DR, Karlson U (1990) Influence of temperature and organic amendments on the mobilization of selenium in sediments. Soil Biology and Biochemistry 22(5): 615–620.https://doi.org/10.1016/0038-0717(90)90006-L

Chen Y-W, Zhou X-L, Tong J, Truong Y, Belzile N (2005) Photochemical behavior of inorganic and organic selenium compounds in various aqueous solutions. Anal. Chim. Acta 545(2): 149-157.https://doi.org/10.1016/j.aca.2005.03.033

Cline JD (1969) Spectrophotometric determination of hydrogen sulfide in natural waters. Limnol. Oceanogr. 14(3): 454–458.https://doi.org/10.4319/lo.1969.14.3.0454

Cooke CA, Holland KM, Emmerton CA, Drevnick PE, Criscitiello AS, Newton B (2024) Mountaintop Removal Coal Mining Contaminates Snowpack across a Broad Region. Environ Sci Technol 58(26): 11718-11726.https://doi.org/10.1021/acs.est.4c02596

Couture R-M, Gobeil C, Tessier A (2008) Chronology of atmospheric deposition of arsenic inferred from reconstructed sedimentary records. Environ. Sci. Technol. 42(17): 6508–6513.https://doi.org/10.1021/es800818j

Couture R-M, Gobeil C, Tessier A (2010) Arsenic, iron and sulfur co-diagenesis in lake sediments. Geochim. Cosmochim. Acta 74(4): 1238–1255.https://doi.org/10.1016/j.gca.2009.11.028

Couture RM, Wallschlager D, Rose J, Van Cappellen P (2013) Arsenic binding to organic and inorganic sulfur species during microbial sulfate reduction: a sediment flow-through reactor experiment. Environ. Chem. 10(4): 285-294.https://doi.org/10.1071/EN13010

Dalai S, Sivan M, Husain MA, Alam N, Landrot G, Biswas A (2023) Mechanistic insight into the abiotic interactions of selenate and selenite with natural organic matter. Environ. Sci. Technol. 57(43): 16595–16605.https://doi.org/10.1021/acs.est.3c06276

Darcheville O, Fevrier L, Haichar FZ, Berge O, Martin-Garin A, Renault P (2008) Aqueous, solid and gaseous partitioning of selenium in an oxic sandy soil under different microbiological states. J Environ Radioact 99(6): 981–992.https://doi.org/10.1016/j.jenvrad.2007.11.006

Davidson EA, Janssens IA, Luo Y (2006) On the variability of respiration in terrestrial ecosystems: moving beyond Q10. Global Change Biol. 12(2): 154–164.https://doi.org/10.1111/j.1365-2486.2005.01065.x

Deen SG, Hendry MJ, Barbour SL, Das S, Essilfie-Dughan J (2022) Removal of dissolved selenium by siderite, pyrite, and sphalerite: Implications to selenium sequestration in water-saturated, anoxic coal waste rock. Geochemistry: 125863.https://doi.org/10.1016/j.chemer.2022.125863

583 Dick RP (2011) Methods of soil enzymology. Soil Science Society of America, Madison

584 Fernández-Martínez A, Charlet L (2009) Selenium environmental cycling and bioavailability: a
585 structural chemist point of view. Rev. Environ. Sci. Bio/Technol. 8(1): 81–
586 110.https://doi.org/10.1007/s11157-009-9145-3

587 Fortin D, Leppard GG, Tessier A (1993) Characteristics of lacustrine diagenetic iron
588 oxyhydroxides. Geochim. Cosmochim. Acta 57(18): 4391–4404.https://doi.org/10.1016/0016-
589 7037(93)90490-N

590 Gabor RS, Baker A, McKnight DM, Miller MP (2014) Fluorescence indices and their
591 interpretation. In: Baker A, Reynolds DM, Lead J, Coble PG & Spencer RGM (eds) Aquatic
592 Organic Matter Fluorescence. Cambridge Environmental Chemistry Series. Cambridge
593 University Press, Cambridge, pp 303–338

594 Gao HH, Chen MX, Hu XQ, Chai SS, Qin ML, Cao ZY (2018) Separation of selenium species
595 and their sensitive determination in rice samples by ion-pairing reversed-phase liquid
596 chromatography with inductively coupled plasma tandem mass spectrometry. J. Sep. Sci. 41(2):
597 432–439.https://doi.org/10.1002/jssc.201700756

598 Goberna-Ferron S, Asta MP, Zareeipolgardani B, Bureau S, Findling N, Simonelli L, Greneche
599 JM, Charlet L, Fernandez-Martinez A (2021) Influence of silica coatings on magnetite-catalyzed
600 selenium reduction. Environ. Sci. Technol. 55(5): 3021–
601 3031.https://doi.org/10.1021/acs.est.0c08146

602 Guida C, Ramothe V, Chappaz A, Simonnin P, Rosso KM, Ding R-R, Prieur D, Scheinost AC,
603 Charlet L (2023) Revisiting selenium interactions with pyrite: from adsorption to coprecipitation.
604 ACS Earth and Space Chem. 8(1): 67–78.https://doi.org/10.1021/acsearthspacechem.3c00219

605 Gustafsson JP, Johnsson L (1992) Selenium retention in the organic matter of Swedish forest
606 soils. Journal of Soil Science 43(3): 461–472.https://doi.org/10.1111/j.1365-2389.1992.tb00152.x

607 Gustafsson JP, Johnsson L (1994) The association between selenium and humic substances in
608 forested ecosystems - laboratory evidence. Appl. Organomet. Chem. 8(2): 141–
609 147.https://doi.org/10.1002/aoc.590080209

610 Hatfield DL, Schweizer U, Tsuji PA, Gladyshev VN (2016) Selenium : its molecular biology and
611 role in human health. In. Springer, New York. p 628

612 Ho MS, Vettese GF, Morris K, Lloyd JR, Boothman C, Bower WR, Shaw S, Law GTW (2022)
613 Retention of immobile Se(0) in flow-through aquifer column systems during bioreduction and
614 oxic-remobilization. Sci Total Environ 834:
615 155332.https://doi.org/10.1016/j.scitotenv.2022.155332

616 Jones ID, Smol JP, Wetzel RG (2024) Wetzel's limnology : lake and river ecosystems. Academic
617 Press, an imprint of Elsevier, London

618 Joshani A, Mirzaei Y, Barber A, Balind K, Gobeil C, Gelinas Y (2024) Organic matter
619 preservation through complexation with iron minerals in two basins of a dimictic boreal lake with
620 contrasting deep water redox regimes. Sci. Total Environ. 925:
621 171776.https://doi.org/10.1016/j.scitotenv.2024.171776

622 Kausch M, Ng P, Ha J, Pallud C (2012) Soil-aggregate-scale heterogeneity in microbial selenium
623 reduction. Vadose Zone J. 11(2): vzj2011.0101.https://doi.org/10.2136/vzj2011.0101

624 Laberge-Carignan A, Pilote M, Larivière D, Mercier F, Folhas D, Couture R-M (2024) Seasonal
625 contrasts in dissolved selenium dynamics in Subarctic thaw lakes. ACS Earth and Space Chem.
626 8(7): 1359–1369.https://doi.org/10.1021/acsearthspacechem.4c00041

LaRowe DE, Van Cappellen P (2011) Degradation of natural organic matter: A thermodynamic analysis. Geochim. Cosmochim. Acta 75(8): 2030–2042.https://doi.org/10.1016/j.gca.2011.01.020

Lenz M, Hullebusch ED, Hommes G, Corvini PF, Lens PN (2008) Selenate removal in methanogenic and sulfate-reducing upflow anaerobic sludge bed reactors. Water Res. 42(8-9): 2184–2194.https://doi.org/10.1016/j.watres.2007.11.031

Li W, Wang T, Boult S (2024) Determining Fe concentration and speciation in waters with high natural organic matter content. Appl. Geochem. 163: 105936.https://doi.org/10.1016/j.apgeochem.2024.105936

Li Z, Liang D, Peng Q, Cui Z, Huang J (2017) Interaction between selenium and soil organic matter and its impact on soil selenium bioavailability: A review. Geoderma 295: 69–79.https://doi.org/10.1016/j.geoderma.2017.02.019

Li Z, Man N, Wang S, Liang D, Liu J (2015) Selenite adsorption and desorption in main Chinese soils with their characteristics and physicochemical properties. J. Soils Sediments 15(5): 1150–1158.https://doi.org/10.1007/s11368-015-1085-7

Liu K, Wu LL, Couture RM, Li WQ, Van Cappellen P (2015) Iron isotope fractionation in sediments of an oligotrophic freshwater lake. Earth Planet. Sci. Lett. 423: 164–172.https://doi.org/10.1016/j.epsl.2015.05.010

Lizotte M, Juhls B, Matsuoka A, Massicotte P, Mével G, Anikina DOJ, Antonova S, Bécu G, Béguin M, Bélanger S, Bossé-Demers T, Bröder L, Bruyant F, Chaillou G, Comte J, Couture R-M, Devred E, Deslongchamps G, Dezutter T, Dillon M, Doxaran D, Flamand A, Fell F, Ferland J, Forget M-H, Fritz M, Gordon TJ, Guilmette C, Hilborn A, Hussherr R, Irish C, Joux F, Kipp L, Laberge-Carignan A, Lantuit H, Leymarie E, Mannino A, Maury J, Overduin P, Oziel L, Stedmon C, Thomas C, Tisserand L, Tremblay J-É, Vonk J, Whalen D, Babin M (2023) Nunataryuk field campaigns: Understanding the origin and fate of terrestrial organic matter in the coastal waters of the Mackenzie Delta region. In. Copernicus GmbH.

López-Toyos L, Rodríguez E, García R, Martínez-Tarazona MR, López-Antón MA (2023) Sorption of selenium(IV) and selenium(VI) onto iron oxide/hydroxide-based carbon materials: Activated carbon and carbon foam. Water 15(19): 3499.https://doi.org/10.3390/w15193499

Luo X, Wang Y, Lan Y, An L, Wang G, Li M, Zheng S (2022) Microbial oxidation of organic and elemental selenium to selenite. Sci. Total Environ. 833: 155203.https://doi.org/10.1016/j.scitotenv.2022.155203

Martin AJ, Kuang C, Wallschlager D (2022) Expansion of the Conceptual Model for the Accumulation of Selenium in Lentic Food Chains to Include Redox-Controlled Generation and Diffusion of Selenite and Dissolved Organo-Selenium Compounds. Environ. Toxicol. Chem. 41(11): 2859-2869. https://doi.org/10.1002/etc.5465

Martin AJ, Simpson S, Fawcett S, Wiramanaden CIE, Pickering IJ, Belzile N, Chen YW, London J, Wallschlager D (2011) Biogeochemical mechanisms of selenium exchange between water and sediments in two contrasting lentic environments. Environ. Sci. Technol. 45(7): 2605–2612.https://doi.org/10.1021/es103604p

Mitchell K, Couture RM, Johnson TM, Mason PRD, Van Cappellen P (2013) Selenium sorption and isotope fractionation: Iron(III) oxides versus iron(II) sulfides. Chem. Geol. 342: 21–28.https://doi.org/10.1016/j.chemgeo.2013.01.017

Negi BB, Sinharoy A, Pakshirajan K (2020) Selenite removal from wastewater using fungal pelleted airlift bioreactor. Environ. Sci. Pollut. Res. 27(1): 992–1003.https://doi.org/10.1007/s11356-019-06946-6

Nielsen G, Coudert L, Janin A, Blais JF, Mercier G (2019) Influence of Organic Carbon Sources on Metal Removal from Mine Impacted Water Using Sulfate-Reducing Bacteria Bioreactors in Cold Climates. Mine Water and the Environment 38(1): 104–118.https://doi.org/10.1007/s10230-018-00580-3

Ohno T (2002) Fluorescence inner-filtering correction for determining the humification index of dissolved organic matter. Environ. Sci. Technol. 36(4): 742–746.https://doi.org/10.1021/es0155276

Oremland RS, Steinberg NA, Maest AS, Miller LG, Hollibaugh JT (1990) Measurement of in situ rates of selenate removal by dissimilatory bacterial reduction in sediments. Environ. Sci. Technol. 24: 1157–1164.https://doi.org/10.1021/es00078a001

Oremland RS, Steinberg NA, Presser TS, Miller LG (1991) Insitu bacterial selenate reduction in the agricultural drainage systems of western Nevada. Applied and Environmental Microbiology 57(2): 615–617.https://doi.org/10.1128/aem.57.2.615-617.1991

Pallud C, Meile C, Laverman AM, Abell J, Van Cappellen P (2007) The use of flow-through sediment reactors in biogeochemical kinetics: Methodology and examples of applications. Mar. Chem. 106(1-2): 256–271.https://doi.org/10.1016/j.marchem.2006.12.011

Pallud C, Van Cappellen P (2006) Kinetics of microbial sulfate reduction in estuarine sediments. Geochim. Cosmochim. Acta 70(5): 1148–1162.https://doi.org/10.1016/j.gca.2005.11.002

Paredez JM, Mladenov N, Galkaduwa MB, Hettiarachchi GM, Kluitenberg GJ, Hutchinson SL (2017) A soil column study to evaluate treatment of trace elements from saline industrial wastewater. Water Sci. Technol. 76(9-10): 2698–2709.https://doi.org/10.2166/wst.2017.413

Parkhurst DL, Appelo CAJ (2013) Description of input and examples for PHREEQC version 3: a computer program for speciation, batch-reaction, one-dimensional transport, and inverse geochemical calculations. In: Techniques and Methods. Reston, VA. p 519

Pi K, Van Cappellen P, Tong L, Gan Y, Wang Y (2023) Loss of selenium from mollisol paddy wetlands of cold regions: Insights from flow-through reactor experiments and process-based modeling. Environ. Sci. Technol. 57(15): 6228–6237.https://doi.org/10.1021/acs.est.3c00011

Poirier N, Sohi SP, Gaunt JL, Mahieu N, Randall EW, Powlson DS, Evershed RP (2005) The chemical composition of measurable soil organic matter pools. Organic Geochemistry 36(8): 1174–1189.https://doi.org/10.1016/j.orggeochem.2005.03.005

Ponton DE, Hare L (2013) Relating selenium concentrations in a planktivore to selenium speciation in lakewater. Environmental Pollution 176: 254-260.https://doi.org/10.1016/j.envpol.2013.01.032

Porcal P, Dillon PJ, Molot LA (2015) Temperature dependence of photodegradation of dissolved organic matter to dissolved inorganic carbon and particulate organic carbon. PLoS One 10(6): e0128884.https://doi.org/10.1371/journal.pone.0128884

Saaltink MW, Rodríguez-Escales P (2022) Modeling the Organic Carbon Oxidation and Redox Sequence Under the Partial-Equilibrium Approach: A Discussion by Means of a Semi-Analytical Solution. Water Resources Research 58(7): https://doi.org/10.1029/2021WR031194

712 Schilling K, Borch T, Rhoades CC, Pallud CE (2019) Temperature sensitivity of microbial Fe(III)
713 reduction kinetics in subalpine wetland soils. Biogeochemistry 142(1): 19-
714 35.https://doi.org/10.1007/s10533-018-0520-4

715 Schilling K, VillaRomero JF, Pallud C (2018) Selenate reduction rates and kinetics across depth
716 in littoral sediment of the Salton Sea, California. Biogeochemistry 140(3): 285–
717 298.https://doi.org/10.1007/s10533-018-0492-4

718 Schladow SG, Lee M, Hürzeler BE, Kelly PB (2002) Oxygen transfer across the air-water
719 interface by natural convection in lakes. Limnol. Oceanogr. 47(5): 1394–
720 1404.https://doi.org/10.4319/lo.2002.47.5.1394

721 Sharma VK, McDonald TJ, Sohn M, Anquandah GAK, Pettine M, Zboril R (2015)
722 Biogeochemistry of selenium. A review. Environ. Chem. Lett. 13(1): 49–
723 58.https://doi.org/10.1007/s10311-014-0487-x

724 Shatilla NJ, Carey SK (2019) Assessing inter-annual and seasonal patterns of DOC and DOM
725 quality across a complex alpine watershed underlain by discontinuous permafrost in Yukon,
726 Canada. Hydrol. Earth Syst. Sci. 23(9): 3571–3591.https://doi.org/10.5194/hess-23-3571-2019

727 Söderlund M, Virkanen J, Holgersson S, Lehto J (2016) Sorption and speciation of selenium in
728 boreal forest soil. J. Environ. Radioact. 164: 220–
729 231.https://doi.org/10.1016/j.jenvrad.2016.08.006

730 Steinberg NA, Oremland RS (1990) Dissimilatory selenate reduction potentials in a diversity of
731 sediment type. Appl. Environ. Microbiol. 56(11): 3550–
732 3557.https://doi.org/10.1128/aem.56.11.3550-3557.1990

733 Thompson A, Parker DR, Amrhein C (2003) Selenate partitioning in field-situated constructed
734 wetland mesocosms. Ecol. Eng. 20(1): 17–30.https://doi.org/10.1016/S0925-8574(02)00145-3

735 Tolu J, Thiry Y, Bueno M, Jolivet C, Potin-Gautier M, Le Hecho I (2014) Distribution and
736 speciation of ambient selenium in contrasted soils, from mineral to organic rich. Sci. Total
737 Environ. 479-480: 93–101.https://doi.org/10.1016/j.scitotenv.2014.01.079

738 VillaRomero JF, Kausch M, Pallud C (2013) Selenate reduction and adsorption in littoral
739 sediments from a hypersaline California lake, the Salton Sea. Hydrobiologia 709(1): 129–
740 142.https://doi.org/10.1007/s10750-013-1443-7

741 Vincent WF, Kumagai M, Couture R-M (2024) Chapter 27 - Sediments and Microbiomes. In:
742 Jones ID & Smol JP (eds) Wetzel's Limnology (Fourth Edition). Academic Press, San Diego, pp
743 893–937

744 Viollier E, Inglett PW, Hunter K, Roychoudhury AN, Van Cappellen P (2000) The ferrozine
745 method revisited: Fe(II)/Fe(III) determination in natural waters. Appl. Geochem. 15(6): 785–
746 790.https://doi.org/10.1016/S0883-2927(99)00097-9

747 Wells M, Stolz JF (2020) Microbial selenium metabolism: a brief history, biogeochemistry and
748 ecophysiology. FEMS Microbiol. Ecol. 96(12): fiaa209.https://doi.org/10.1093/femsec/fiaa209

749 Wilson HF, Xenopoulos MA (2009) Effects of agricultural land use on the composition of fluvial
750 dissolved organic matter. Nat. Geosci. 2(1): 37–41.https://doi.org/10.1038/ngeo391

751 Winkel LH, Johnson CA, Lenz M, Grundl T, Leupin OX, Amini M, Charlet L (2012)
752 Environmental selenium research: from microscopic processes to global understanding. Environ.
753 Sci. Technol. 46(2): 571–579.10.1021/es203434d

754 Yan S, Cheng KY, Ginige MP, Zheng G, Zhou L, Kaksonen AH (2020) High-rate microbial
755 selenate reduction in an up-flow anaerobic fluidized bed reactor (FBR). Sci. Total Environ. 749:
756 142359.https://doi.org/10.1016/j.scitotenv.2020.142359

757